

# Thursday Morning, November 1, 2012

## Thin Film

Room: 11 - Session TF+NS+EM-ThM

### Thin Films: Growth and Characterization-II

Moderator: C. Vallee, LTM - MINATEC - CEA/LETI, France

8:00am **TF+NS+EM-ThM1 Plasma-enhanced Atomic Layer Epitaxy of AlN Films on GaN, N. Nepal, J.K. Hite, N. Mahadik, M.A. Mastro, C.R. Eddy, Jr.**, U.S. Naval Research Laboratory

AlN and its alloys with GaN and InN are of great interest for number of applications. In a device structure that employs an ultrathin layer of these materials, thickness control at the atomic scale is essential. Atomic layer epitaxy (ALE) is one of the most promising growth methods for control of epilayer thickness at the atomic scale. There are reports on atomic layer deposition of AlN on GaN and Si substrates [1]. In those reports, the AlN layers were either amorphous or composed of nm-sized crystallites. Since ALE is a low temperature growth process, there is significantly reduced thermal energy for adatoms to bond at preferred lattice sites and promote growth of crystalline material, therefore, surface preparation plays a very important role to ensure a crystalline layer.

In this work, we present recent efforts to improve the crystalline quality of ALE AlN layers on MOCVD grown GaN/sapphire templates, including the influence of *ex situ* and *in situ* surface pretreatments to promote uniform two-dimensional (2D) nucleation of AlN layers and ALE growth of crystalline AlN films thereupon. AlN layers were grown at 500 °C by ALE simultaneously on Si(111) and GaN/sapphire templates and characterized using spectroscopic ellipsometry (SE), x-ray diffraction (XRD), and atomic force microscopy measurements. The SE measurements indicate that the AlN growth on Si(111) is self-limited for trimethylaluminum (TMA) pulse of length 0.04 to 0.06 sec. However, the AlN nucleation has a bimodal island size distribution for TMA pulses < 0.06 sec. The AlN nucleation becomes uniform and 2D for a pulse length of 0.06 sec, therefore, this pulse length was used to study the GaN surface pretreatment on the nucleation of AlN layer. GaN surfaces were pre-treated *ex situ* with HF and HCl wet chemical etches. Alternating pulses of trimethylgallium and hydrogen plasma followed by an hour of annealing at 500 °C (emulating a Ga-flash-off process) were employed *in situ* before growing an AlN layer. For 3 cycles of Ga-flash-off the AlN nucleation is uniform and replicates the GaN surface morphology on both HF and HCl pretreated GaN. XRD measurements on 36 nm thick AlN films reveal that the ALE AlN on GaN/sapphire is crystalline with only a wurtzite structure and a (0002) peak rocking curve FWHM of 630 arc-sec, which is close to the typical value for AlN grown by MBE and MOCVD [2,3]. Electrical characterization of 2D electron gas at the AlN/GaN interface will also be presented.

#### References:

1. M. Alevli et al., Phys. Status Solidi A **209**, 266 (2012), and references therein.
2. T. Koyama et al., Phys. Stat. Sol. (a) **203**, 1603 (2006).
3. K. Balakrishnan et al., Phys. Stat. Sol. (c) **3**, 1392 (2006).

8:20am **TF+NS+EM-ThM2 In Situ Infrared Spectroscopy Study of Cobalt Silicide Thin Film Growth by Atomic Layer Deposition, K. Bernal Ramos**, University of Texas at Dallas, M.J. Saly, SAFC Hitech, J. Kwon, University of Texas at Dallas, M.D. Halls, Materials Design Inc., R.K. Kanjolia, SAFC Hitech, Y.J. Chabal, University of Texas at Dallas

Cobalt silicide has potential applications in microelectronics. For instance, the drive to scale down integrated circuitry (IC) has led to the consideration of cobalt silicide (CoSi<sub>2</sub>) as an alternative contact material for titanium silicide (TiSi<sub>2</sub>) in future self-aligned silicide technology due to its wider silicidation window and superior thermal and chemical stability. Studies of the growth mechanisms during film deposition are critical to better understand and control thin film formation.

This work focuses on the atomic layer deposition (ALD) of cobalt silicide (CoSi<sub>2</sub>), using (tertiarybutylallyl)cobalttricarbonyl ((tBuAllyl)Co(CO)<sub>3</sub>) and trisilane on H-terminated silicon to uncover the film growth mechanisms. The first pulse of (tBuAllyl)Co(CO)<sub>3</sub> reacts completely with the H-terminated Si surface forming one monolayer of metallic silicide through the reduction of the allyl ligand by transfer of the surface hydrogen and the formation of Co-Si bonds. In situ infrared absorption spectra show the complete loss of H-Si bonds, and the appearance of surface-bound carbonyl and CH<sub>x</sub> ligands after the first (tBuAllyl)Co(CO)<sub>3</sub> pulse on H/Si(111). Further deposition of CoSi<sub>2</sub> is possible only after the linear

carbonyl groups (initially observed, on the surface after the first (tBuAllyl)Co(CO)<sub>3</sub>) are removed by subsequent ALD cycles. Further ALD cycles give rise to cobalt silicide growth through ligand exchange after a nucleation period of 2–4 cycles. The resultant CoSi<sub>2</sub> films are characterized by a low concentration of carbon impurities in the bulk according to X-ray photoemission spectroscopy (XPS).

1 Kwon et al. Chem. Mater. 2012, 24, 1025–1030

8:40am **TF+NS+EM-ThM3 Thin Film Growth: From Gas Phase to Solid Phase – Links and Control, P. Raynaud**, CNRS and University Paul Sabatier – Toulouse – France **INVITED**

PECVD, PVD, ALD, sputtering processes, are widely used for thin film growth. Nevertheless, the growth mechanisms need to be controlled and understood to be able to propose stable, adaptable and reproducible processes. Gas, plasma or "volume" phase is one parameter; interaction with surfaces to be treated is the second one, the last one being the final property (ies) to be reached. The Gas phase is controlled by external parameters (pressure, power, polarization, temperature, gas mixture, type of power supply in plasma processes, type of target, duty cycle,). Moreover, these external parameters are linked to internal parameters such as: density and energy of species, type of species (neutrals, ions, electrons, radicals, photons ...), temperature, bombardment energy... Thus, interaction with surfaces and growth process (growth mode, growth rate...) are obviously controlled by these internal parameters and the couple "Gas phase/surface (nature of substrate)". The purpose of this talk is to explain through examples (In situ Infrared spectroscopy of gas phase, OES, MS, Growth modes characterization by in situ ellipsometry, RBS, ARXPS...) how to characterize (in or ex situ) the gas phase et solid phase to find links between these two phases and give some explanation of the processes "from power supply to final properties of the layer".

9:20am **TF+NS+EM-ThM5 Investigation of Precursor Infiltration and ALD Growth on Polymers and Effect on Fiber Mechanical Properties, R.P. Padbury, J.S. Jur**, North Carolina State University

Atomic layer deposition (ALD) provides the opportunity to unite the properties of organic fiber forming polymers and nanoscale inorganic films creating a hybrid material interface. Prior research has shown that ALD materials nucleation on polymers varies in composition and structure based on how the precursor interacts with the polymer chemistry and the process conditions. The purpose of this work is to explore the effect of this processing on the mechanical behavior of fibrous materials. To study this in more detail, *in-situ* quartz crystal microgravimetry (QCM) is employed to understand the material growth mechanisms of ALD TiO<sub>2</sub>, ZnO, and Al<sub>2</sub>O<sub>3</sub> on poly (acrylic acid), polyamide-6, and polyethylene terephthalate. Particular emphasis is placed on controlling the ALD precursor diffusion into the sub-surface region of these polymers. *In-situ* QCM data was complemented by *ex-situ* characterization methods such as FT-IR and TEM to examine the interaction between the precursor and polymer and the compositions of the inorganic films. Finally, these results are correlated to the mechanical performance of the ALD treated fabrics. This work has important implications on sustainable textiles processes as well as the introduction of hybrid material properties to textile systems.

9:40am **TF+NS+EM-ThM6 Atomic Layer Deposition Enabled Synthesis of Nanostructured Composite BiFeO<sub>3</sub>/CoFe<sub>2</sub>O<sub>4</sub> Thin Films for Multiferroic Applications, C.D. Pham, J.P. Chang**, University of California at Los Angeles

Multiferroic materials, that can either exist as single-phase materials or multi-phase composites, exhibit two or more forms of ferroic order such as (anti)ferroelectricity, (anti)ferromagnetism, or ferroelasticity and have been proposed for use in future non-volatile memory technology. Atomic layer deposition (ALD) is proposed as a scalable approach to synthesize multiferroic thin films and to enable the synthesis of multiferroic composites which utilize conformal deposition onto 3-D nanostructures. Challenges that must be overcome in the ALD of multiferroic materials is the amorphous nature of as-deposited films and the difficulty in attaining the desired crystallinity and structure that would enable multiferroic properties to emerge from these materials.

In this work, multiferroic BiFeO<sub>3</sub> was deposited by ALD as a single-phase multiferroic thin film as well as the ferroelectric component in a composite multiferroic using a ferrimagnetic CoFe<sub>2</sub>O<sub>4</sub> mesoporous template that was synthesized using an evaporation induced di-block copolymer self-assembly technique. The ALD process used the metallorganic precursors Bi(tmhd)<sub>3</sub> (tmhd = 2,2,6,6-tetramethylheptane-3,5 dione) and Fe(tmhd)<sub>3</sub> alongside oxygen atoms produced from a coaxial waveguide microwave powered

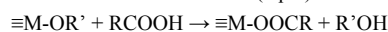
atomic beam source. A variety of ALD process conditions were studied, such as the effects of process temperature, precursor pulsing time, and precursor pulsing ratio on film composition, growth rate, and crystallization. The ALD films were able to be grown with a composition ratio Bi:Fe close to unity and with a controlled nanostructure and growth rate of  $\sim 0.7$  Å/cycle. In order to achieve the desired crystalline material after rapid thermal processing, the composition and nanostructure of the as-deposited films must first be controlled via the ALD process to fit within narrow windows.

To compare the performance of the multiferroic ALD films to more well established synthesis methods, measurements of magnetic and ferro/piezoelectric properties were accomplished using SQUID magnetometry and piezoresponse force microscopy, respectively. Magnetic measurements showed that the out-of-plane remnant magnetization of a composite film at room temperature was approximately  $66.4 \text{ emu/cm}^3$  while the coercive field was approximately 1950 Oe which was comparable to epitaxial films grown by other methods such as PLD. The magnetoelectric coupling effects in the composite films were studied to assess the effectiveness of the nanostructured material approach.

10:40am **TF+NS+EM-ThM9 In Situ Infrared Spectroscopic Study of Atomic Layer Deposited TiO<sub>2</sub> Thin Film Formation Using Non-Aqueous Routes**, *K. Bernal Ramos*, University of Texas at Dallas, *G. Clavel*, Université Montpellier 2, France, *C. Marichy*, Universidade de Aveiro / CICECO, Portugal, *W. Cabrera*, The University of Texas at Dallas, *N. Pinna*, Universidade de Aveiro / CICECO, Portugal, *Y.J. Chabal*, University of Texas at Dallas

Atomic layer deposition (ALD) is a unique technique for the deposition of conformal and homogenous thin films, by the use of successive self-limited surface reactions. Non-aqueous sol-gel routes are elegant approaches for the synthesis of metal oxide nanomaterials.<sup>1</sup> High quality inorganic nanocrystals,<sup>1</sup> ordered hybrid materials<sup>2</sup> or ALD thin films<sup>3</sup> can be obtained.

Our ALD approach makes use of metal alkoxides and carboxylic acids as metal and oxygen source, respectively.<sup>4</sup> It is expected that the reaction of carboxylic acids with the surface alkoxide species leads to surface carboxylate species (eq. 1), in a second step an aprotic condensation reaction between surface carboxylate species and metal alkoxides leads to metal-oxide bond formation (eq. 2).



Characterization of interface properties by in situ investigation of surface reaction mechanisms during deposition of high-*k* materials provides critical information for the development of semiconductor devices, where sharp interfaces and impurity free films are sought after.

In this work, in-situ IR spectroscopy is used to investigate the mechanisms for TiO<sub>2</sub> growth using either acetic acid or O<sub>3</sub> as oxygen source and titanium isopropoxide as metal source. It is believed to avoid intermediate OH group and to lead to sharp Si-high-*k* interfaces.

The IR results of the acetic acid process show clearly a ligand exchange leading to formation of acetates at the surface (vibrational bands at 1527 and 1440 cm<sup>-1</sup>) during the acetic acid pulse and then to their removal during the metal alkoxide pulse. These findings confirm the expected mechanism and demonstrate the absence of OH intermediate. However, the ligand exchange does not seem to be complete leading to accumulation of C impurities.

The in-situ study of O<sub>3</sub> based ALD demonstrates similarities with the above process. Indeed, formation of formate, carboxylate or carbonate species are observed function of the O<sub>3</sub> flow.<sup>5</sup> The formation of surface carboxylic species upon reaction with O<sub>3</sub> leads then to similar surface states as in the case of the reaction with carboxylic acids.<sup>4</sup> The mechanism of both approaches and their similarities and differences will be discussed.

1. N. Pinna and M. Niederberger, *Angew. Chem.-Int. Edit.*, 2008, **47**, 5292-5304

2. N. Pinna, *J. Mater. Chem.*, 2007, **17**, 2769-2774

3. G. Clavel, E. Rauwel, M. G. Willinger and N. Pinna, *J. Mater. Chem.*, 2009, **19**, 454-462

4. E. Rauwel, G. Clavel, M. G. Willinger, P. Rauwel and N. Pinna, *Angew. Chem.-Int. Edit.*, 2008, **47**, 3592-3595

5. J. Kwon, M. Dai, M. D. Halls, E. Langereis, Y. J. Chabal and R. G. Gordon, *J. Phys. Chem. C*, 2009, **113**, 654-660

11:00am **TF+NS+EM-ThM10 Nanomechanical Shaft-Loading Blister Testing of Thin Films**, *M. Berdova*, *A. Baby*, *J. Lyytinen*, Aalto University, Finland, *K. Grigoros*, *L. Kilpi*, *H. Ronkainen*, VTT Technical Research Center, Finland, *J. Koskinen*, *S. Franssila*, Aalto University, Finland

Atomic Layer Deposition (ALD) is important in micro- and nano-electromechanical systems, since it provides smooth, uniform, pin-hole free, and conformal layers. In particular, ALD aluminum oxide has excellent properties such as high mechanical strength and hardness, and chemical inertness.

We propose a new technique to measure the mechanical properties of ALD thin films. In the present work, a MEMS version shaft-loading blister test used to evaluate the adhesion between ALD alumina and Cu, Cr/Cu, SiN<sub>x</sub>, SiC<sub>x</sub>, and Pt thin films. The test structure consists of microcylinders with diameters 1000 μm and 2000 μm, surrounded by etched annular rings making 50 μm, 100 μm and 200 μm gaps (Figure 1). The test structures are examined by applying the load along the microcylinder with a help of CSM Microindenter, inducing displacement which then causes the delamination between thin films and therefore, contributing to obtain the work of adhesion (Figure 2).

The fabrication of the test structure begins from the cleaning of double-side polished silicon wafer in hydrogen-peroxide-based (RCA) wet cleans. The following step is Atomic Layer Deposition of alumina on both sides of the wafer using trimethyl aluminium and water as precursors at 220 °C. 20 nm of Al<sub>2</sub>O<sub>3</sub> is grown on one side as the etch mask, and 200 nm of Al<sub>2</sub>O<sub>3</sub> is grown on another side to act both as an etch-stop mask and a testing layer. Next, the top layer is patterned to create alumina etch mask; and the rings are etched through silicon wafer by dry anisotropic Bosch process, forming this way a microcylinders supported only by 200 nm of Al<sub>2</sub>O<sub>3</sub> layer. Then, thin films (300 nm thick) are deposited by sputtering, or by PECVD techniques. The silicon nitride and silicon carbide were deposited at 300 °C. Magnetron sputtering was used for deposition of Pt, Cu, and Cr/Cu thin films at room temperature. Finally, those films are released by wet etching supporting alumina layer around the microcylinder.

As a result, we have not observed the delamination for nitride and carbide films: after certain reached displacement point (7 μm for nitride, 12 μm for carbide) the films start to break. For soft films as Pt and Cu, at similar displacement values we observed the starting of delamination. Comparing copper and copper with chromium layer underneath, the delamination of the film with adhesive layer starts at higher displacement and load values, proving the adhesive action of chromium. In the case of metal films large displacement and delamination can be achieved without breaking of the film (Table 1). The proposed MEMS shaft-loading blister test might become a valuable tool for all thin film adhesion testing.

11:20am **TF+NS+EM-ThM11 Phase Formation and Thermal Stability of Arc-Evaporated ZrAlN Thin Films**, *L. Rogström*, Linköping University, Sweden, *M.P. Johansson*, SECO Tools AB, Sweden, *M. Ahlgren*, Sandvik Tooling AB, Sweden, *N. Ghafoor*, Linköping University, Sweden, *J. Almer*, Advanced Photon Source, Argonne National Lab, *L. Hultman*, *M. Odén*, Linköping University, Sweden

Transition metal nitrides are widely used as wear protective coatings due to their high hardness also at elevated temperatures. Hence, TiAlN is one of the most common materials for coating of cutting tools. Its attractive mechanical properties are connected with the phase separation of the cubic TiAlN phase when the coating is exposed to high temperatures. The related ZrAlN system is less studied while its large miscibility gap with possibility for phase separation at elevated temperatures makes this material interesting for high temperature applications. Here, we present a comprehensive study of the phase formation in arc-evaporated ZrAlN thin films and their mechanical properties and thermal stability. Zr<sub>1-x</sub>Al<sub>x</sub>N thin films with a wide range of compositions (0.12 < x < 0.73) were grown by cathodic arc-evaporation. The structure of as-deposited and annealed films was characterized by x-ray diffraction and transmission electron microscopy and the mechanical properties were determined by nanoindentation.

The structure of the as-deposited ZrAlN thin films was found to depend on the Al-content. A low Al-content (x < 0.38) results in cubic (c) structure films while for high Al-content (x > 0.70) a hexagonal (h) ZrAlN phase is obtained [1]. In the compositional range between x = 0.38 and x = 0.70, the films exhibit a nanocomposite structure with a mixture of cubic, hexagonal, and amorphous phases [1, 2]. In all films, separation of ZrN and AlN takes place during annealing. In films with a nanocomposite structure, the phase transformation is initiated by nucleation and growth of c-ZrN in the ZrN-rich domains while the AlN-rich domains remain largely amorphous at 1100 °C [3]. Nucleation and growth of h-AlN is hindered by a high nitrogen content in the film and takes place at annealing above 1300 °C, simultaneously to loss of the excess nitrogen. The depletion of amorphous phase during annealing results in an improved hardness of the film. In the h-ZrAlN films, ZrN- and AlN-rich domains form within the hexagonal lattice during annealing above 900 °C. The formation of domains with different

composition results in an increased hardness, from 24 GPa of the as-deposited film to 31 GPa of the annealed film. The *c*-ZrAlN phase is found to be stable to annealing temperatures of 1000 °C, while at higher temperatures, *h*-AlN nucleates and grows. This is different from the *c*-TiAlN system where spinodal decomposition occurs resulting in age hardening of the films.

[1] L. Rogström et al., J. Vac. Sci. Technol. A 30 (2012) 031504.

[2] L. Rogström et al., Scr. Mater. 62 (2010) 739.

[3] L. Rogström et al., J. Mater. Res., In press (2012)

11:40am **TF+NS+EM-ThM12 Ion-assisted Epitaxial Sputter-Deposition and Properties of Metastable  $Zr_{1-x}Al_xN(001)$  (0.05 x 0.25) Alloys**, *AR.B. Mei, B.M. Howe*, University of Illinois at Urbana Champaign, *N. Ghafour, E. Broitman*, Linköping University, Sweden, *M. Sardela*, University of Illinois at Urbana Champaign, *L. Hultman*, Linköping University, Sweden, *A. Rockett, J.E. Greene, I. Petrov*, University of Illinois at Urbana Champaign, *M. Oden, H. Fager*, Linköping University, Sweden

Single-phase epitaxial metastable  $Zr_{1-x}Al_xN/MgO(001)$  ( 0.05 x 0.25 ) thin films were deposited by ultra-high vacuum magnetically-unbalanced reactive magnetron sputtering from a single  $Zr_{0.75}Al_{0.25}$  target at a substrate temperature of 650°C. We control the AlN content,  $x$ , in the films by varying the ion energy ( $5 < E_i < 55$  eV) incident at the film growth surface with a constant ion to metal flux ratio of 8. The net atomic flux was decreased from  $3.16$  to  $2.45 \times 10^{15}$  atoms  $cm^{-2}s^{-1}$ , due to efficient resputtering of deposited Al atoms (27 amu) by Ar<sup>+</sup> ions (40 amu) neutralized and backscattered from heavy Zr atoms (91.2 amu). Consequentially, films varied in thickness from 400 nm to 290 nm during 20 min depositions. HfN buffer layers were deposited on the MgO(001) substrates to reduce the lattice mismatch from ~8 to ~0.5%. High resolution x-ray diffraction  $\omega$ -2 $\theta$  scans and reciprocal lattice mapping revealed single-phase NaCl structure with a cube-on-cube orientation relative to the substrate,  $(001)_{Zr_{1-x}Al_xN} \parallel (001)_{MgO}$ , and relaxed lattice parameters varying from 4.546 Å with  $x = 0.25$  to 4.598 Å with  $x = 0.05$ . Film nanoindentation measurements showed that hardness decreases from 28.6 to 23.3 GPa and Young's modulus increases from 263 GPa to 296.8 GPa as  $x$  is varied from 0.25 to 0.05. For the same range in  $x$ , electronic transport measurements established the films to have electron mobilities increasing from 2.67 to 462  $cm^2V^{-1}s^{-1}$ , resistivities decreasing from 162.4 to 25.4  $\mu\Omega$ -cm, and positive temperature coefficients of resistivity spanning from 0.3164 to 1.307  $\Omega$ -cm  $K^{-1}$ . Films deposited with incident ion energy above 35 eV ( $x < 0.08$ ) exhibited superconductivity with  $T_c$  of 8.26 K.

# Authors Index

**Bold page numbers indicate the presenter**

## — A —

Ahlgren, M.: TF+NS+EM-ThM11, **2**  
Almer, J.: TF+NS+EM-ThM11, **2**

## — B —

Baby, A.: TF+NS+EM-ThM10, **2**  
Berdova, M.: TF+NS+EM-ThM10, **2**  
Bernal Ramos, K.: TF+NS+EM-ThM2, **1**;  
TF+NS+EM-ThM9, **2**  
Broitman, E.: TF+NS+EM-ThM12, **3**

## — C —

Cabrera, W.: TF+NS+EM-ThM9, **2**  
Chabal, Y.J.: TF+NS+EM-ThM2, **1**; TF+NS+EM-ThM9, **2**  
Chang, J.P.: TF+NS+EM-ThM6, **1**  
Clavel, G.: TF+NS+EM-ThM9, **2**

## — E —

Eddy, Jr., C.R.: TF+NS+EM-ThM1, **1**

## — F —

Fager, H.: TF+NS+EM-ThM12, **3**  
Franssila, S.: TF+NS+EM-ThM10, **2**

## — G —

Ghafoor, N.: TF+NS+EM-ThM11, **2**; TF+NS+EM-ThM12, **3**

Greene, J.E.: TF+NS+EM-ThM12, **3**  
Grigoras, K.: TF+NS+EM-ThM10, **2**

## — H —

Halls, M.D.: TF+NS+EM-ThM2, **1**  
Hite, J.K.: TF+NS+EM-ThM1, **1**  
Howe, B.M.: TF+NS+EM-ThM12, **3**  
Hultman, L.: TF+NS+EM-ThM11, **2**;  
TF+NS+EM-ThM12, **3**

## — J —

Johansson, M.P.: TF+NS+EM-ThM11, **2**  
Jur, J.S.: TF+NS+EM-ThM5, **1**

## — K —

Kanjolia, R.K.: TF+NS+EM-ThM2, **1**  
Kilpi, L.: TF+NS+EM-ThM10, **2**  
Koskinen, J.: TF+NS+EM-ThM10, **2**  
Kwon, J.: TF+NS+EM-ThM2, **1**

## — L —

Lyytinen, J.: TF+NS+EM-ThM10, **2**

## — M —

Mahadik, N.: TF+NS+EM-ThM1, **1**  
Marichy, C.: TF+NS+EM-ThM9, **2**  
Mastro, M.A.: TF+NS+EM-ThM1, **1**  
Mei, A.R.B.: TF+NS+EM-ThM12, **3**

## — N —

Nepal, N.: TF+NS+EM-ThM1, **1**

## — O —

Oden, M.: TF+NS+EM-ThM12, **3**  
Odén, M.: TF+NS+EM-ThM11, **2**

## — P —

Padbury, R.P.: TF+NS+EM-ThM5, **1**  
Petrov, I.: TF+NS+EM-ThM12, **3**  
Pham, C.D.: TF+NS+EM-ThM6, **1**  
Pinna, N.: TF+NS+EM-ThM9, **2**

## — R —

Raynaud, P.: TF+NS+EM-ThM3, **1**  
Rockett, A.: TF+NS+EM-ThM12, **3**  
Rogström, L.: TF+NS+EM-ThM11, **2**  
Ronkainen, H.: TF+NS+EM-ThM10, **2**

## — S —

Saly, M.J.: TF+NS+EM-ThM2, **1**  
Sardela, M.: TF+NS+EM-ThM12, **3**